Excitation of States in Pb^{207} by $Pb^{208}(d,t)$, $Pb^{206}(d,p)$, and $Pb^{207}(d,d')$ Reactions*

R. A. Moyer,† B. L. Cohen, and R. C. Diehl‡
University of Pittsburgh, Pittsburgh, Pennsylvania 15213
(Received 12 June 1970)

States up to 5.6 MeV in excitation energy in Pb^{207} were studied by the $Pb^{208}(d,t)$, $Pb^{206}(d,p)$, and $Pb^{207}(d,d')$ reactions at a deuteron bombarding energy of 17 MeV. Over 100 states were observed and 70 angular distributions were measured and compared with distorted-wave Born approximation calculations for the (d,p) and (d,t) reactions. Special emphasis was placed on obtaining accurate excitation energies to compare those states excited in more than one reaction. In $Pb^{206}(d,p)$, some of the two-hole–one-particle (2h-1p) states are found to be fragmented. The $i_{11/2}$ and $j_{15/2}$ 2h-1p states are tentatively identified. Many of the weaker (less than 5 μb/sr) transitions in (d,t) have angular distributions which do not follow DWBA – possibly indicating other than one-step reaction mechanisms. Observation of the 2h-1p states in (d,t) indicate that the Pb^{208} closed shell contains about 4.7% $(2g_{9/2})^2$, $\lesssim$4.7% $(3d_{5/2})^2$, and $\lesssim$1.2% $(4s_{1/2})^2$ particle-Pb^{206} core admixture.

I. INTRODUCTION

In the nucleus Pb^{208}, both the 82 protons and 126 neutrons form closed shells. Pb^{208} and surrounding nuclei seem to follow the predictions of the shell model surprisingly well.[1,2] Unlike the ground states of lighter closed-shell nuclei which contain significant admixtures, the Pb^{208} ground state appears to be a very good closed shell. This paper attempts to give the amount of two-hole–two-particle (2h-2p) components for neutrons in the ground state of Pb^{208}.

The level density is very high in the lead region necessitating the use of a stable high-resolution accelerator and particle detection system. The University of Pittsburgh three-state tandem Van De Graaff accelerator and Enge split-pole spectrograph satisfy these requirements.

The neutron single-particle (1p) and single-hole (1h) levels near $N=126$ are shown in Fig. 1. By performing (d,p) experiments on Pb^{206} (two neutron holes removed from Pb^{208}), the lowest-energy two-hole–one-particle (2h-1p) states of Pb^{207} in which the neutrons are paired can be identified. The same 2h-1p states are then looked for in the $Pb^{208}(d,t)Pb^{207}$ reaction. If any 2h-1p states are seen, they are indicative of 2h-2p admixtures in the ground state of Pb^{208}. Although there have been previous studies of Pb^{207}, no direct comparison between reactions from Pb^{206} and Pb^{208} leading to Pb^{207} has been made.

The 2h-1p states in the (d,t) reaction are expected to be very weak. Thus, very long exposures must be made. Since the states of interest extend up to 5.3 MeV in excitation, a special effort was made to obtain an accurate calibration of the Enge split-pole spectrograph. A $Pb^{207}(d,d')Pb^{207}$ experiment was also performed in hopes of tieing together the energy levels seen in the (d,p) and (d,t) experiments.

In $Pb^{206}(d,p)Pb^{207}$ the 2h-1p states appear to be somewhat fragmented. An attempt was made to locate these fragments and the missing $i_{11/2}$ and $j_{15/2}$ 2h-1p states.

II. EXPERIMENTAL

In all three experiments the incident beam was 17-MeV deuterons from the University of Pittsburgh three-stage Van de Graaff accelerator. The scattered particles were detected by photographic emulsions after magnetic analysis in an Enge split-pole spectrograph. The beam handling system has been described in a previous paper.[3]

Complete angular distributions were measured for both the (d,p) and (d,t) reactions leading to states of Pb^{207}. Data were taken at eight angles in the (d,t) reaction – 30, 45, 60, 75, 90, 115, 130, and 144°. The (d,p) angular distributions showed more structure, so 15 angles were observed – 6, 8, 10, 12, 14, 20, 28, 35, 45, 60, 75, 90, 115, 130, and 144°. In the (d,d') reaction which was taken as a check on excitation energies, data were obtained at only three angles – 60, 75, and 90°.

Isotopically enriched targets evaporated onto thin (30 μg/cm^2) carbon foils were used. Enrichments were as follows: Pb^{208} – 99.47%, Pb^{207} – 92.40%, and Pb^{206} – 97.39%.

Isotopic impurities for each reaction studied were eliminated from the spectra by exposing a natural Pb target at one or more angles and eliminating peaks in the enriched spectrum due to other isotopes. Light-element impurities could be distinguished from peaks of interest by their relative shift as a function of angle and by the fact that they are kinematically defocused by the spectrograph.

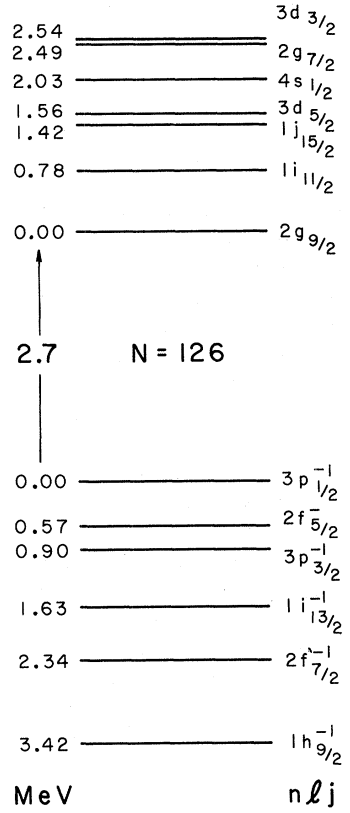

FIG. 1. Experimental single-particle and single-hole neutron levels and energies in the $N=126$ region. Single-particle data are taken from the levels of Pb^{209} while the single-hole and gap data are taken from the levels of Pb^{207}.

Unfortunately, these broad light-element impurity peaks obscured peaks of interest at several angles resulting in the gaps seen in the angular distributions. These impurities are especially prevalent at small angles.

Since the states studied in (d,t) are weakly excited, it was decided to give up some energy resolution in order to obtain higher counting rates. This was done by increasing the solid angle of the spectrograph (to 2.83 msr) and using thick targets. Typical length of exposure was 3 h with 0.5 μA of beam. For the (d,t) reaction, the Pb^{208} target thicknesses were 1.2 mg/cm^2 for angles less than 100° and 0.31 mg/cm^2 for angles greater than 100°. Resolution varied from 16 to 28 keV full width at half maximum (FWHM).

In the $Pb^{206}(d,p)$ reaction two different targets were used – 20 and 130 μg/cm^2. Resolution varied between 8 and 18 keV. The spectrograph solid angle was reduced to the normal 1.4 msr for high-resolution exposures, permitting the observation of several doublets not seen with poorer resolution. Peaks which were weak on the high-resolution exposure (as in Fig. 2) were observed with good intensity by using thicker targets. By comparing relative intensities of thick and thin targets at the same angle, some peaks due to heavy-element surface impurities were thus eliminated.

The target thickness for the $Pb^{207}(d,d')$ reaction was 400 μg/cm^2. With the normal spectrograph solid angle, typical resolution was 10 keV.

The beam was monitored with NaI(Tl) scintillation detectors at ±38°. The Pb elastic deuteron peak in the monitors was used to calculate the cross section for the peaks appearing on the photographic emulsions. To do this, it is necessary to

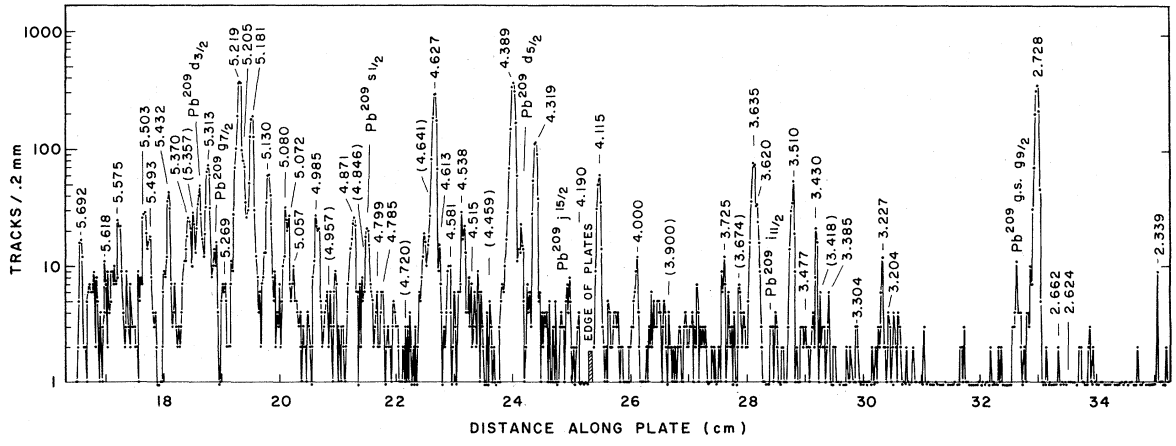

FIG. 2. $Pb^{206}(d,p)Pb^{207}$ spectrum above 2.3 MeV at a lab scattering angle of 130°. Tracks per 0.2 mm are plotted on a logarithmic scale. Numbers above peaks are the excitation energy of the corresponding level in Pb^{207}. Also indicated are the single-particle states from the $Pb^{208}(d,p)Pb^{209}$ reaction. Numbers in parentheses indicate that the state is questionable.

know the relative solid angles and the cross section for elastic scattering of deuterons by Pb at 38° and 17 MeV. The latter can be easily measured if the thickness of one Pb target is known. By lowering the beam energy to 9 MeV where elastic scattering at 38° was assumed to be completely Rutherford, the target thickness was determined. Absolute cross sections are probably accurate to about 15% for this work.

A great deal of effort was expended to obtain an accurate calibration for the Enge split-pole spectrograph. This is essential because of the high excitation energies observed in this work and the necessity to correlate the (d,p) and (d,t) levels to determine the 2h-2p components in the ground state of Pb^{208}.

An obvious method immediately comes to mind. By keeping the beam at a constant energy and the spectrograph at a fixed angle, one could step the magnetic field of the spectrograph to move an elastic peak along the plate and, thus, generate a ρ versus L curve, where L is the distance along the plate and ρ is the radius of curvature of the particle in the magnetic field. This was done and a least-squares program was used to fit the data to a polynomial in L. As a check, one can use different beam energies or different elastic particles to obtain the same ρ-versus-L curve for different ranges in the magnetic field of the spectrograph. Curves for three ranges of magnetic field (as measured by an NMR probe) *did not agree*. Thus, the ρ versus L curve is dependent on the value of the magnetic field.

Since the magnetic field is varied in the above method, it is *not* a suitable method for an accurate calibration. The deviation of the curves is larger than in comparable single-pole magnets and may be due to the split-pole nature of the spectrograph.

Another method of calibration was used. The energy uncertainty of the first four excited states in Pb^{207} up to 2.3393 MeV known from γ-ray studies,[4] is less than 1 kV. By performing (d,p), (d,d'), or (d,t) reactions exciting these states in Pb^{207}, one can obtain a calibration for a fixed magnetic field. Adjusting the beam energy, one can generate a series of these five peaks along the plate and thus obtain a ρ versus L curve. Care was taken to account for energy loss due to target thickness and kinematic effects. Any uncertainty in the beam energy as well as Q value is carried over into the calibration. An attempt was made to adjust for these uncertainties by smoothing the data across

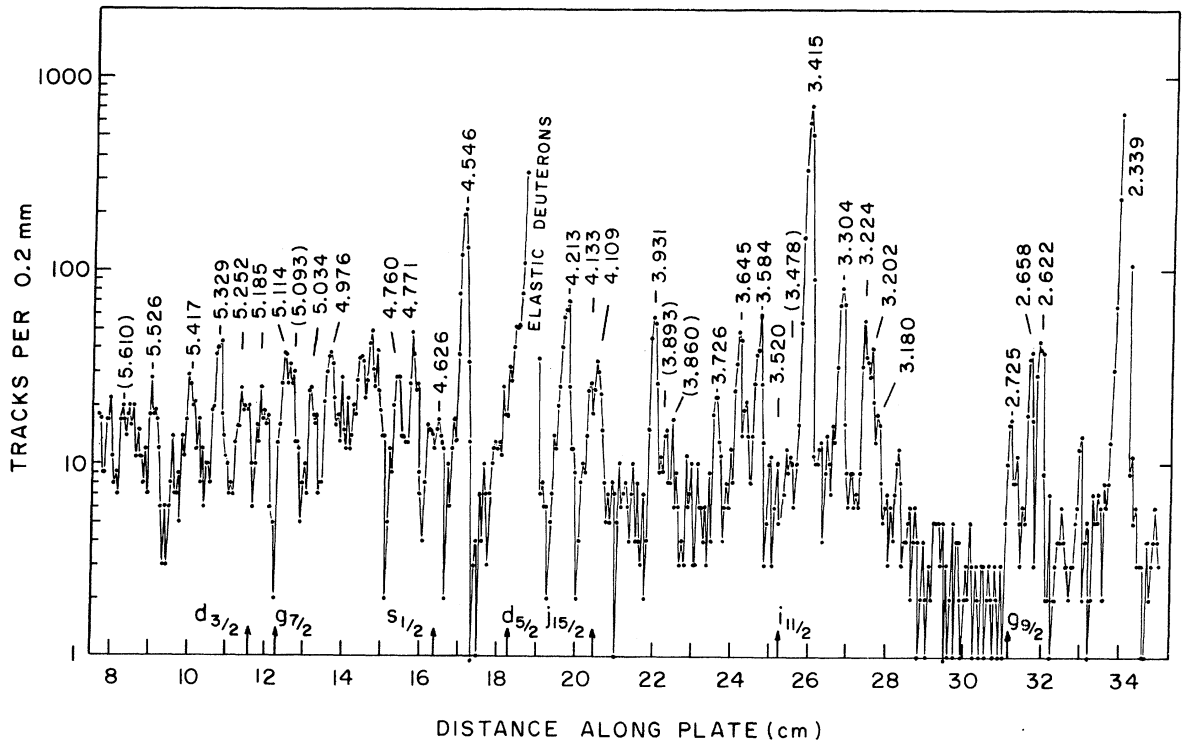

FIG. 3. $Pb^{208}(d,T)Pb^{207}$ spectrum above 2.3 MeV at a lab scattering angle of 130°. Tracks per 0.2 mm at 0.5-mm intervals are plotted on a logarithmic scale. Numbers above peaks are the excitation energy of the corresponding level in Pb^{207}. Triton peaks above the deuteron elastic are clearly resolved. Arrows at bottom of figure indicate the expected location of the 2h-1p states.

variations in beam energy.

The final calibration was obtained by least-squares-fitting the data for (d,p), (d,d'), and (d,t) at three different energies. The uncertainty in excitation energy for this method is 0.4%. The uncertainty of the calibration data was noticeably larger at the high-ρ end of the plate (high L, and low excitation energies in this experiment). To reduce the error in excitation energies, all energies in this experiment are adjusted to make the energy of the 2.3393 level correct. Thus, errors in states above 2.3393 are relative to that state.

It was noted that the peaks shifted up to a mm if the beam-analyzing magnet and spectrograph were recycled and put on a fixed hysteresis loop. This was in spite of the fact that both fields are set using an NMR probe. The calibration and all data were obtained using a fixed recycling procedure which was established.

The excitation energies quoted in this paper have

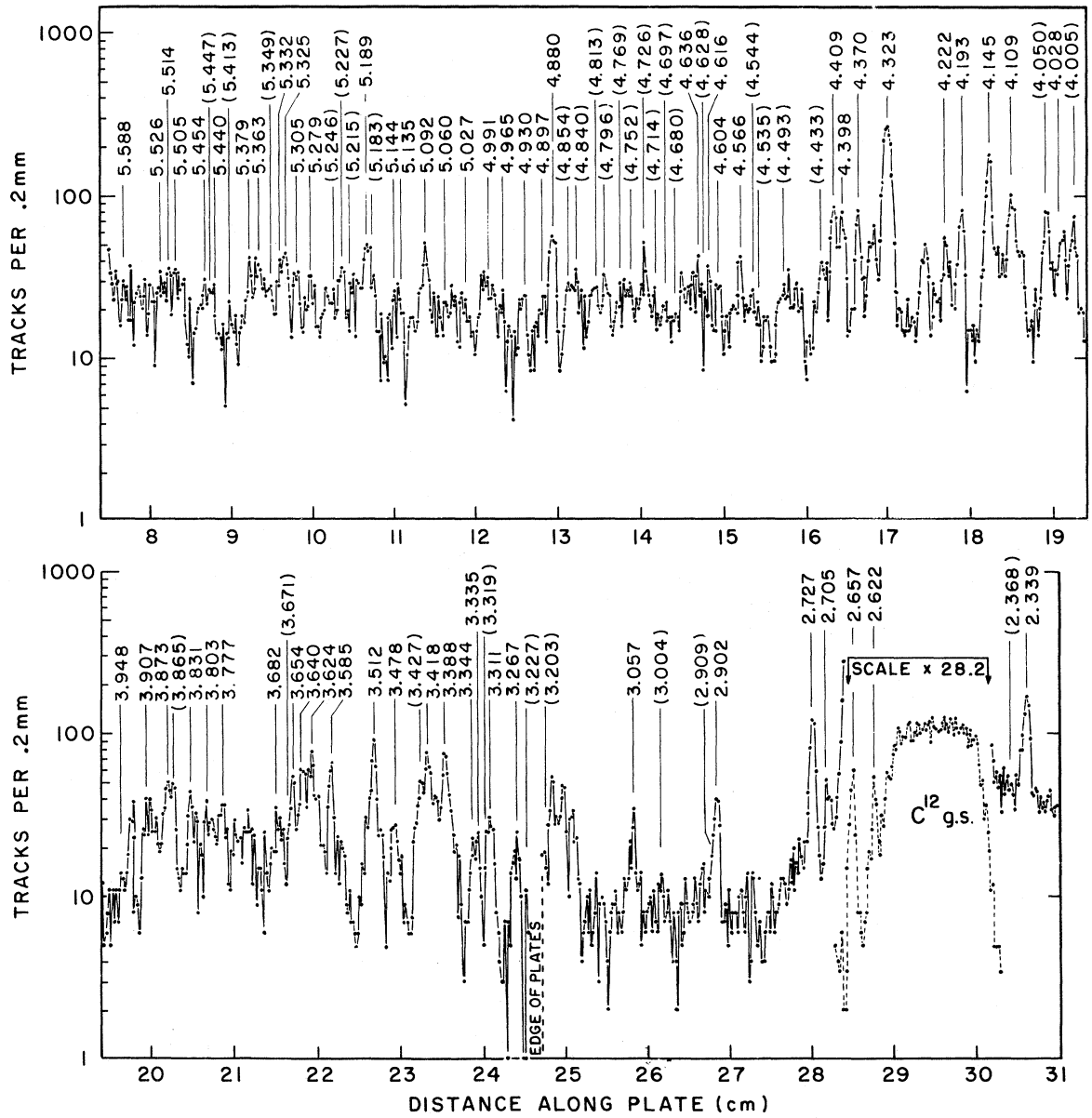

FIG. 4. $Pb^{207}(d,d')Pb^{207}$ spectrum above 2.3 MeV at a lab scattering angle of 60°. Tracks per 0.2 mm are plotted on a logarithmic scale. Numbers above peaks are the excitation energy of the corresponding level in Pb^{207}. Data points connected by a dashed line are from a shorter exposure. Numbers in parentheses indicate that the state is questionable.

been corrected for energy loss of the incident beam and scattered particle in the target. To obtain the best resolution, the focal plane must be shifted to account for $dE/d\theta$ of the scattered particle as the spectrograph angle is changed. The excitation energies have also been corrected for this shift in the focal plane. For the high excitation energies studied in these reactions, it was necessary to use spectra which covered two photographic plates. In all cases, the gap between the plates was measured and the excitation energies were corrected.

III. RESULTS AND ANALYSIS

A. General

Typical energy spectra of emitted particles are shown in Figs. 2, 3, and 4. The arrows in Fig. 3 indicate where in the $Pb^{208}(d,t)Pb^{207}$ spectrum the 2h-1p states are expected. If seen, these states indicate 2h-2p components in the ground state of Pb^{208}. The position of these arrows is determined from the location of the 2h-1p states observed in $Pb^{206}(d,p)Pb^{207}$.

Table I lists the energies, maximum cross sections, possible assignments, and corresponding spectroscopic factors of states observed in Pb^{207} via (d,p), (d,t), and (d,d') reactions. Also listed are the $Pb^{207}(p,p')Pb^{207}$ results of Vallois[5] at 24.5 MeV.

All Pb^{207} states between 2.3 and 5.6 MeV listed in Table I are plotted in Fig. 5. The height of each line represents the maximum cross section for the reaction indicated. I^{π} assignments are shown above several states. Assignments for the (d,d') are taken from Vallois's thesis[5] by comparing the present (d,d') results with the (p,p') reported there.

Figure 5 shows that, in general, states which are strong in (d,p) are weak or not detected in (d,t) and vice versa. For excitation energies below 3.5 MeV, several states are detected in all three reactions at very nearly the same energy. These are believed to be the same states in Pb^{207}. Table I lists such states on the same line. Above 3.5 MeV, the lineup of states from different reactions is less clear because of difficulties in the spectrograph calibration (discussed in Sec. II). States which have energies close enough and which vary in a consistent manner are listed on the same line throughout Table I.

The theoretical distorted-wave Born approximation[6](DWBA) predictions are plotted on the right side of Figs. 6 and 7. Optical-model parameters (listed in Table II) were obtained from $Pb^{208}(d,p)$ and $Pb^{208}(d,t)$ by Muehllehner, Poltorak, Parkinson, and Bassel.[7] The imaginary volume absorption potential W_0 for the triton in (d,t) was interpolated to a 17-MeV beam energy. The fits to both the 2h-1p states (Fig. 8) observed in the $Pb^{206}(d,p)$ reaction and the single-hole states (Fig. 7) observed in the $Pb^{208}(d,t)$ reaction are good. Thus, no attempt was made to adjust the parameters to obtain improved fits to the present data.

The shape of the DWBA angular distributions is sensitive to the excitation energy of the transition being fitted. The (d,t) distributions are more sensitive, since for high excitation energy the triton energy is close to that of the Coulomb barrier. Even though the proton is above the barrier, the low-l angular distributions do change appreciably with excitation energies.

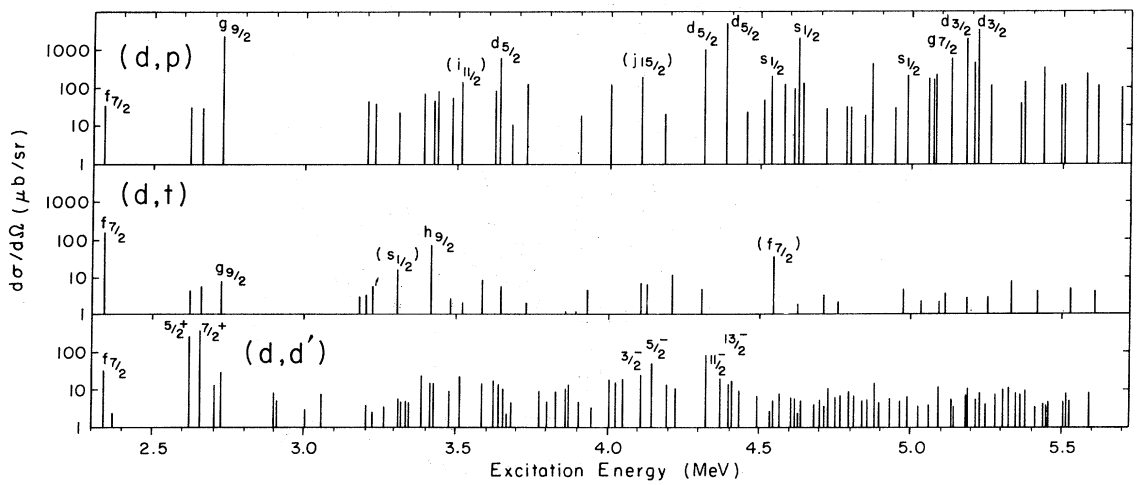

FIG. 5. States in Pb^{207} observed between 2.3 and 5.6 MeV in the three reactions studied (d,p), (d,t), (d,d'). The maximum cross section listed in Table I is represented by the height of each line plotted on a multicycled logarithmic scale. l_j or I^{π} assignments are shown above some of the states. Assignments for (d,d') are taken from Ref. 5.

TABLE I. Results for Pb^{207}.

States excited in Pb^{207} by			l or I^π assignment from				$\frac{d\sigma}{d\Omega}$ (Ref. a)		Spectroscopic factor from			Vallois's energy assignments (Ref. b)	
(d,p)	(d,t)	(d,d')	(d,p)		(d,t)		(d,p)	(d,t)	(d,d')	(d,p)	(d,t)	(p,p')	l or I^π
0.0		0.0	1	$\frac{1}{2}^-$			0.871		119.7	0.60			
0.571	0.575	0.572	3	$\frac{5}{2}^-$	3	$\frac{5}{2}^-$	0.144	2.038	0.065	0.12	6.8	0.568	(2)
0.898	0.899	0.899	1	$\frac{1}{2}^-$	1	$\frac{3}{2}^-$	0.230	3.654	0.071	0.069	4.0	0.895	(2)
1.633	1.634	1.632	(6)	$\frac{13}{2}^+$	6	$\frac{13}{2}^+$	0.023	0.353	0.010	(0.015)	14.5	1.632	(7)
2.339[c]	2.339[c]	2.339[c]	(3)	$(\frac{7}{2}^-)$	3	$\frac{7}{2}^-$	(0.069)	1.087	0.036	(0.016)	7.1	2.338	$\frac{7}{2}^-$
		(2.368)							0.003				
2.624	2.622	2.622	if	$\frac{5}{2}^+$	if	$\frac{5}{2}^+$	0.079	0.005	0.288	(0.006)	(0.014)	2.627	$\frac{5}{2}^+$
2.662	2.658	2.657	if	$\frac{7}{2}^+$	if	$\frac{7}{2}^+$	(0.037)	0.006	0.396	(0.031)	(0.006)	2.668	$\frac{7}{2}^+$
		2.705							0.015				
2.728	2.725	2.727	4	$\frac{9}{2}^+$	4	$\frac{9}{2}^+$	2.208	0.009	0.033	0.97	0.091	2.736	(5)
		2.902							0.009				
		(2.909)							0.005[d]				
		(3.004)							0.003				
		3.057[e]							0.008				
	3.180							0.004					
3.204	3.202	(3.203)					0.012	0.004	0.004				
3.227	3.224	(3.227)					0.025	0.006	0.003				
		3.267							0.004				
3.304	3.304					$\frac{1}{2}^+(\frac{9}{2}^-)$	0.021	0.018			0.055(1.9)		
		3.311							0.006				
		(3.319)							0.005				
		3.335							0.005				
		3.344							0.005				
3.385		3.388					0.027		0.025			3.381	5
(3.418)	3.415	3.418	if	$\frac{9}{2}^-$	5	$\frac{9}{2}^-$	0.048	0.089	0.017	(0.02)	9.8	3.407	4
		(3.427)							(0.016)			3.428	(6)
3.430							0.069						
3.477	(3.478)	3.478	1,4				0.023	0.003	0.009			3.468	
3.510		3.512		$\frac{11}{2}^+$ $(\frac{15}{2}^-)$			0.107		0.023	0.48(0.75)		3.506	(6)
	3.520							0.002					
	3.584	3.585[f]						0.009	0.015			3.577	5
3.620		3.624					0.088		0.020			3.614	5
3.635		3.640	2	$\frac{5}{2}^-$			0.677		0.015	0.14		3.641[g]	
	3.645				2,3,4,5			0.006					
		3.654							0.010			3.641[g]	
		(3.671)							0.002				
(3.674)							(0.015)						
		3.682							0.006				
3.725	3.726		2,3				0.133	0.002				3.712	
		3.777							0.009			3.766	
		3.803							0.005				
		3.831							0.009			3.817	
	(3.860)							0.001					
		(3.865)							0.010			3.854[g]	(3)
		3.873							0.015			3.854[g]	(3)
	(3.893)							0.001					
(3.900)							0.024						
		3.907							0.005			3.891	
	3.931							0.005					
		3.948							0.003				
4.000			2,3				0.106						
		(4.005)							0.018			3.989	
		4.028							0.016				
		(4.050)							0.019				

TABLE I *(Continued)*

States excited in Pb^{207} by			l or I^π assignment from		$\frac{d\sigma}{d\Omega}$ (Ref. a)		Spectroscopic factor from			Vallois's energy assignments (Ref. b)	
(d,p)	(d,t)	(d,d')	(d,p)	(d,t)	(d,p)	(d,t)	(d,d')	(d,p)	(d,t)	(p,p')	l or I^π
	4.109	4.109				0.007				4.089	$\frac{3}{2}^-$
4.115			$\frac{15}{2}^-$ $(\frac{11}{2}^+)$		0.212			1.45(0.89)			
	4.133					0.007					
		4.145					0.045			4.127	$\frac{5}{2}^-$
4.190		4.193	0,1,4,5		0.020		0.015			4.181	
	4.213			2,3,4,5		0.013					
		4.222					0.012			4.215	
	4.311					0.005					
4.319		4.323	2 $\frac{5}{2}^+$		1.136		0.089	0.19		4.288	4
		4.370					0.019			4.339	$\frac{11}{2}^-$
4.389	4.386?		2 $\frac{5}{2}^+$	if $\frac{5}{2}^+$	4.430	(0.004)		0.77	(0.072)		
		4.398					0.015			4.380[g]	$\frac{13}{2}^-$
		4.409					0.020			4.380[g]	$\frac{13}{2}^-$
		(4.433)					0.010				
(4.459)					0.026						
		(4.493)					0.007				
4.515			2 $\frac{5}{2}^+$		0.044			0.075			
		(4.535)					0.003				
4.538			0 $\frac{1}{2}^+$		0.218			0.085			
		(4.544)					0.005				
	4.546			(3 $\frac{7}{2}^-$)		(0.065)			(1.4)		
		4.566					0.008				
4.581			$\frac{5}{2}^+$ $(\frac{7}{2}^-)$		0.142			0.023(0.019)			
		4.604					0.007				
4.613		4.616			0.104		0.006				
4.627	4.626	(4.628)	0 $\frac{1}{2}^+$	if $\frac{1}{2}^+$	2.210	0.002[h]	0.003	1.09	(0.028)	4.615[g]	(8)
		4.636					0.005			4.615[g]	(8)
(4.641)					0.156						
		(4.680)					0.004				
		(4.697)					0.005				
	4.711	(4.714)				0.003	0.004				
(4.720)					0.014						
		(4.726)					0.011				
		(4.752)					0.007				
	4.760					0.003					
		(4.769)					0.007				
4.785					0.036						
		4.796					0.009				
4.799					0.031						
		(4.813)					0.008				
		(4.840)					0.005				
(4.846)					(0.012)						
		(4.854)					0.006				
4.871			$\frac{5}{2}^+, \frac{7}{2}^-, \frac{7}{2}^+$		0.266		i				
		4.880					0.016				4.865
		4.897					0.005				
		4.930					0.006				
(4.957)					(0.031)						
		4.965					0.005				
	4.976					0.004[h]					
4.985			0 $\frac{1}{2}^+$		0.028			0.095			
		4.991					0.007				
		(5.027)					0.004				
	5.034					0.002[h]					
5.057		5.060	4,2,3		0.186		0.004				

TABLE I *(Continued)*

States excited in Pb^{207} by			l or I^π assignment from		$\frac{d\sigma}{d\Omega}$ (Ref. a)		Spectroscopic factor from			Vallois's energy assignments (Ref. b)	
(d,p)	(d,t)	(d,d')	(d,p)	(d,t)	(d,p)	(d,t)	(d,d')	(d,p)	(d,t)	(p,p')	l or I^π
5.072					0.160						
5.080			4,2,3		0.209						
		5.092					0.011				
	(5.093)					0.004[h]					
	5.114					0.004[h]					
5.130			4 $\frac{7+}{2}$		0.602			0.018			
		5.135					0.005				
		5.144					0.004				
5.181		(5.183)	2 $\frac{3+}{2}$		1.842		0.007	0.25			
	5.185	5.189				0.003[h]	0.010				
5.205			4,2,3		0.483						
		(5.215)					0.006				
5.219			2 $\frac{3+}{2}$		3.674			0.53			
		(5.227)					0.009				
		(5.246)					0.004				
	5.252					0.003[h]					
5.269					0.113						
		5.279					0.008				
		5.305					0.010				
5.313			$\frac{7+}{2}, \frac{3+}{2}$		0.710			(0.14,0.10)			
		5.325					0.013				
	5.329	5.332				0.005[h]	0.008				
		(5.349)					0.008				
(5.357)		5.363			(0.040)		0.007				
5.370					0.145						
		5,379					0.009				
		(5.413)					0.003				
	5.417					0.003[h]					
5.432			$\frac{7+}{2}, \frac{3+}{2}$		0.343			(0.11,0.061)			
		5.440					0.005				
		(5.447)					0.004				
		5.454					0.005				
5.493					0.116						
5.503		5.505			(0.214)		0.006				
		5.514					0.008				
	5.526	5.526				0.003[h]	0.005				
5.575		5.588	$\frac{3+}{2}, \frac{7-}{2}, \frac{7+}{2}$		0.259		0.008	i			
	(5.610)										
5.618					0.123						
5.692			$\frac{7+}{2}, \frac{3+}{2}$		0.096			(0.026,0.015)			

[a] In mb/sr, measured at first peak beyond 12°, except for (d,d') which was measured at 60°.
[b] From Ref. 5.
[c] Spectra normalized to this energy.
[d] Obscured at 60°, value for 75°.
[e] Possibly a doublet.
[f] May be isotopic impurity.
[g] Were not resolved in Ref. 5.
[h] Below elastic deuteron peak, largest of values at 115, 130, or 144°.
[i] See Fig. 8 for spectroscopic factors.

As can be seen from the right side of Fig. 6, j values cannot be distinguished by comparison to DWBA angular distributions. Whenever possible, tentative j values are assigned based on the known level structure (Fig. 1) for neutrons on both sides of the 126 closed shell. Figures 9, 10, and 11 show the probable DWBA curves drawn through the experimental data points and extracted spectroscopic factors. For certain excitation energies, it is very difficult to distinguish between $l=2$ and

$l = 3$ distributions. Uncertainty is introduced into l-value assignments, since only a limited number of angles were measured, and at some angles peaks of interest were obscured by impurities.

Spectroscopic factors were calculated using the cross section of the first peak in the experimental angular distribution and comparing it with the DWBA cross section. The usual definition of spectroscopic factors was used

$$\frac{d\sigma}{d\Omega}(d,p) = 1.5(2j+1)S\sigma_{\mathrm{DWBA}}(\theta)\ ,$$

$$\frac{d\sigma}{d\Omega}(d,t) = 3.33S\sigma_{\mathrm{DWBA}}(\theta)\ ,$$

where S is the spectroscopic factor, j is the total angular momentum of the transferred neutron, and $\sigma_{\mathrm{DWBA}}(\theta)$ is the DWBA cross section at the peak.

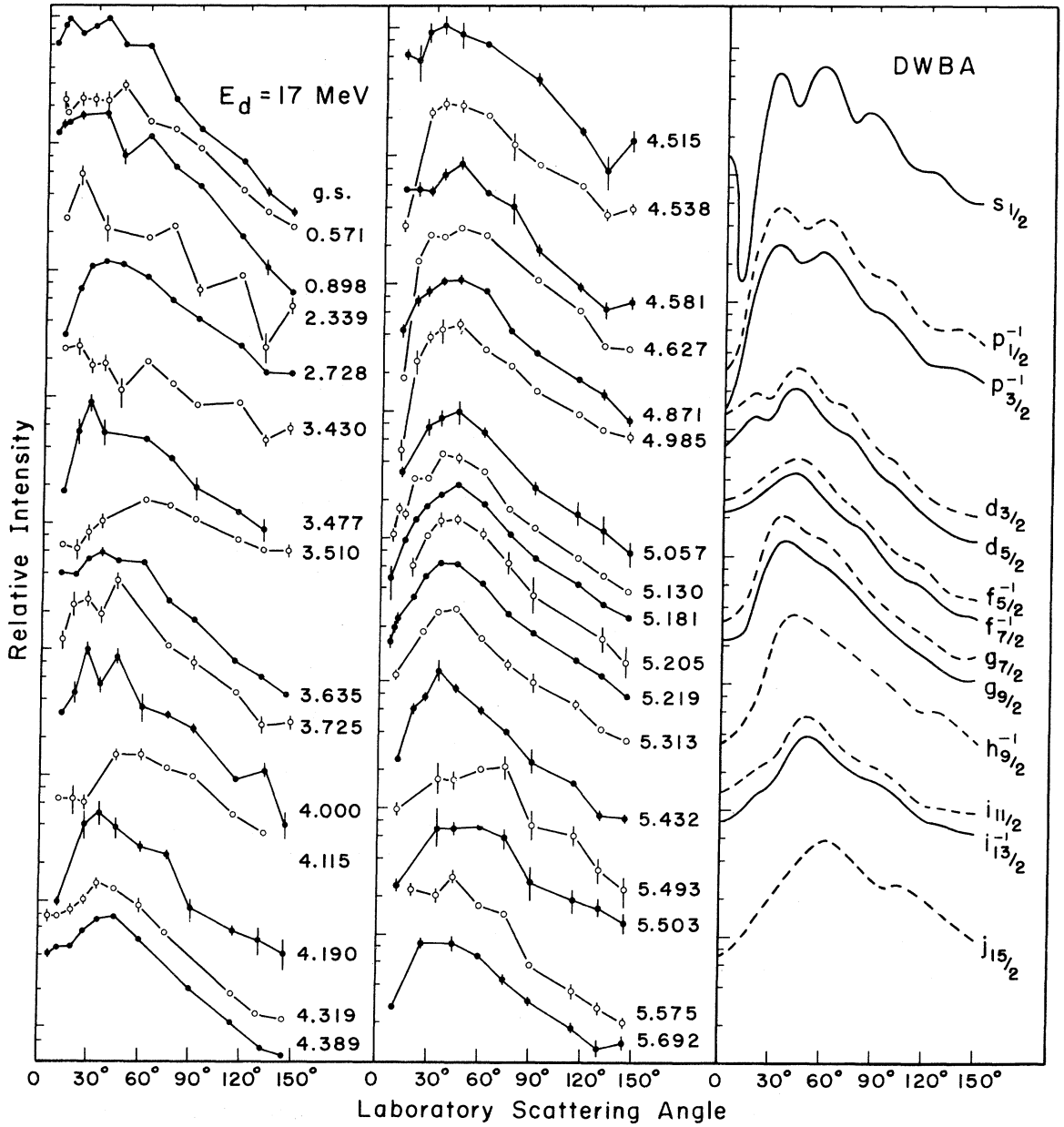

FIG. 6. Experimental and DWBA angular distributions for $Pb^{206}(d,p)Pb^{207}$. Lines through the data points are to aid the eye. Numbers to the right of the experimental curves are the excitation energies in MeV. All DWBA curves are for an excitation energy of 5.0 MeV. Error bars include statistical errors as well as those due to peak limiting and background subtraction.

The $g_{9/2}$ spectroscopic factor obtained in the $Pb^{206}(d,p)Pb^{207}$ reaction using the above formula and parameters of Table II is low by nearly 30%. Using a natural-lead target, the intensity of this peak and the Pb^{209} $g_{9/2}$ ground state were compared. The two intensities are equal to within 5% and hence their spectroscopic factors are equal within this percentage. It is generally assumed that the $g_{9/2}$ ground state of Pb^{209} is a good single-particle state and hence has a spectroscopic factor near unity. This is based on the fact that there is very little[8] $g_{9/2}$ strength in the spectrum of Pb^{209} other than the ground state. Thus, the spectroscopic factor for the $g_{9/2}$ state observed in Pb^{207} must also be near unity.

Using a natural-lead target at one angle (60°), all $Pb^{208}(d,p)Pb^{209}$ single-particle spectroscopic factors (listed in Table III) were normalized to uni-

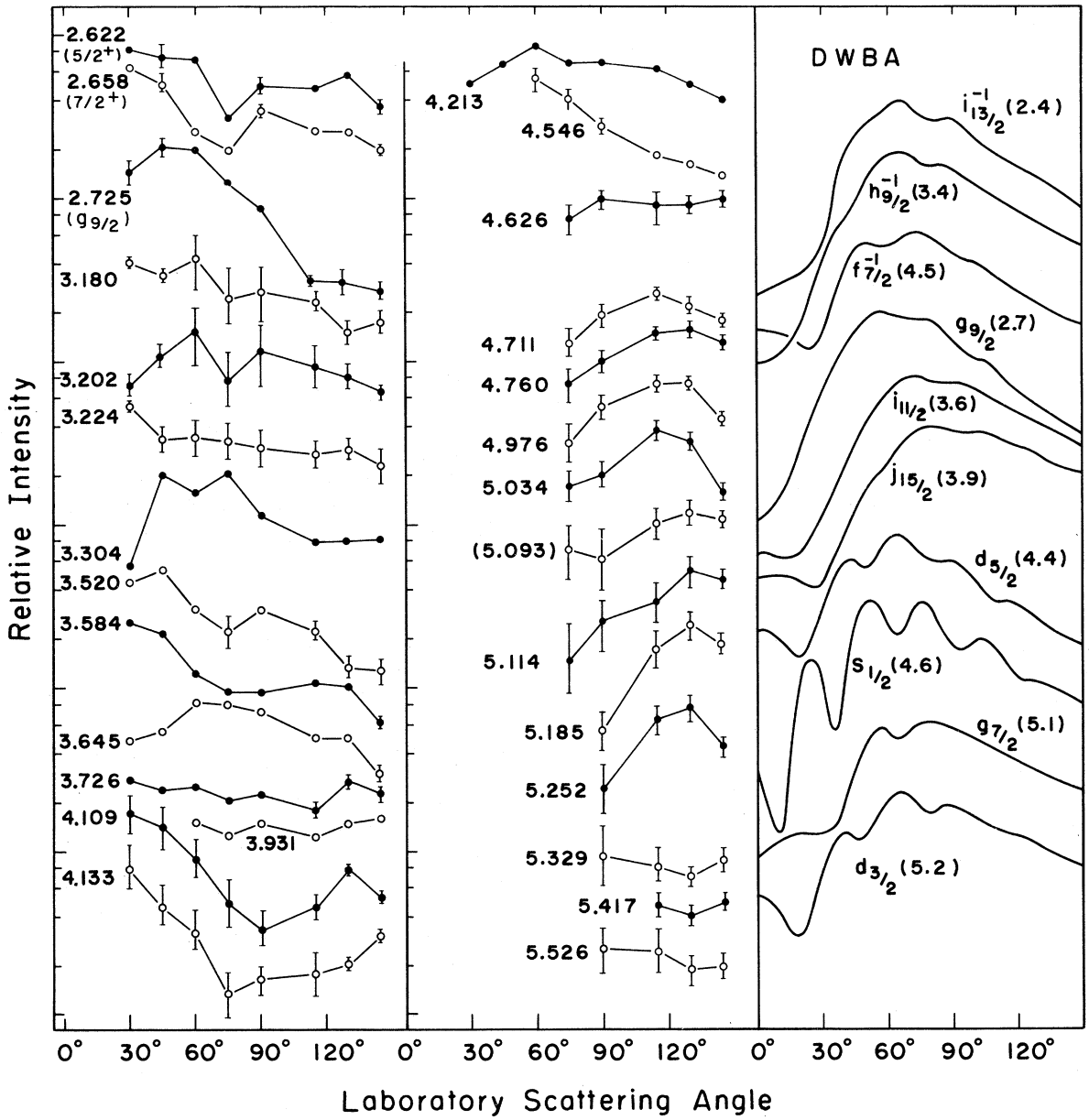

FIG. 7. Experimental and DWBA triton angular distributions for the $Pb^{208}(d,t)Pb^{207}$ reaction. Lines through the experimental points are to aid the eye. Numbers to the left of the experimental curves are the excitation energies in MeV. Numbers to the right of the DWBA curves are the excitation energies in MeV for which the calculation was performed. Error bars include statistical errors and those due to peak limiting.

TABLE II. Optical-model parameters used in the DWBA calculations (from Ref. 7).

Reaction	V_0 (MeV)	r_0 (fm)	r_C (fm)	a (fm)	W_0 (MeV)	r_0' (fm)	a' (fm)	W_D (MeV)	V_{so} (MeV)	λ
					Deuteron					
$Pb^{206}(d,p)$	100.0	1.14	1.30	0.89	0.0	1.33	0.75	13.8	0.0	
					Neutron					
$Pb^{206}(d,p)$	a	1.20		0.65						25
					Proton					
$Pb^{206}(d,p)$	52.0	1.25	1.25	0.65	0.0	1.25	0.76	7.5	0.0	
					Deuteron					
$Pb^{208}(d,t)$	100.0	1.14	1.30	0.89	0.0	1.33	0.75	13.8	0.0	
					Neutron					
$Pb^{208}(d,t)$	a	1.225		0.70						25
					Triton					
$Pb^{208}(d,t)$	168.0	1.14	1.4	0.723	18.0	1.52	0.77	0.0	0.0	

[a] Calculated by JULIE to give the binding energy of the neutron.

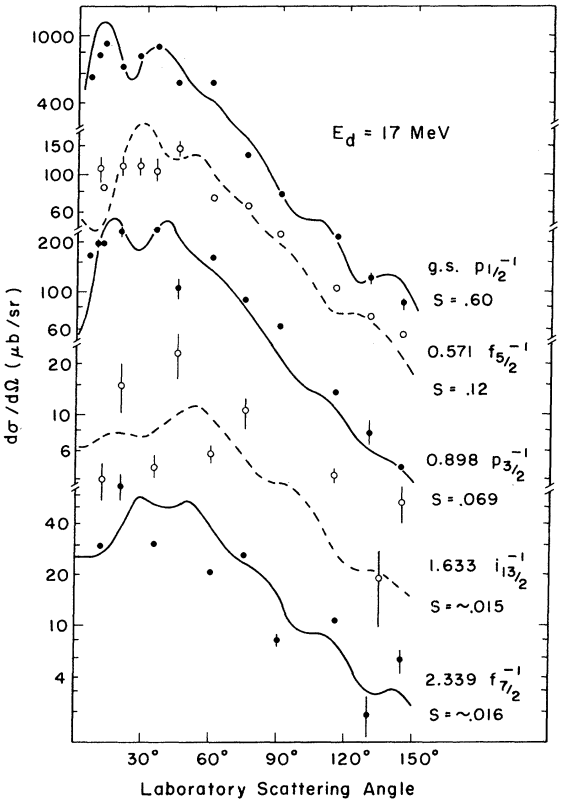

FIG. 8. Angular distributions for protons from Pb^{206}-$(d,p)Pb^{207}$ leading to the single-hole states in Pb^{207}: Lines through the data points are the calculated DWBA curves for that excitation energy. S is the extracted spectroscopic factor. Error bars are as in Fig. 6.

ty. The $j_{15/2}$ level at 1.424 MeV in Pb^{209} appears to be fragmented ($S \approx 0.5$) as found by several researchers.[9-11] Thus, the normalizing factor listed in Table III for this state is about double what it is for the other states.

All 2h-1p spectroscopic factors obtained from parameters of Table II for $Pb^{206}(d,p)Pb^{207}$ given in this work have been multiplied by the normalizing factors listed in Table III. Those for $j_{15/2}$ states, as mentioned above, are probably too high. The *single-hole* spectroscopic factors were not changed, since no normalizing procedure could be established, if needed. No attempt was made to adjust the parameters given in Table II to obtain more accurate fits or spectroscopic factors. The (d,t) spectroscopic factors were not changed, as the values obtained for the single-hole states are quite close to the expected values $(2j+1)$.

Hering, Achterath, and Dost[12] have done Coulomb (d,p) stripping and obtained spectroscopic factors for several levels in Pb^{207}. Table IV compares their results with the present work. The spectroscopic factors agree quite closely except for the 5.181-MeV state, which will be discussed later. The total spectroscopic factor for the three $s_{1/2}$ states seen in this work equals 1.27. This is within the typical error of 30% for spectroscopic-factor determination for this work.

B. $Pb^{206}(d,p)Pb^{207}$

Although there was only 1.92% Pb^{208} in the Pb^{206} target, the strong single-particle states of Pb^{209} were detected in the $Pb^{206}(d,p)Pb^{207}$ reaction. The

TABLE III. Pb^{209} single-particle spectroscopic factors and factors necessary to normalize to unity. DWBA parameters from Table II.

State	Spectroscopic factor	Normalizing factor
$g_{9/2}$	0.68	1.47
$i_{11/2}$	0.81	1.23
$j_{15/2}$	0.39 [a,b]	2.59
$d_{5/2}$	0.65 [b]	1.53
$s_{1/2}$	0.52 [b]	1.92
$g_{7/2}$	0.93	1.07
$d_{3/2}$	1.13	0.88

[a] This level is probably fragmented and has $S \approx 0.5$ as found in Refs. 9, 10, and 11.

[b] Somewhat questionable (±20%) due to interfering peaks.

seven Pb^{209} single-particle states are labeled in Fig. 2. Unfortunately, the intensity of these peaks was not enough to give accurate angular distributions. This prohibited a comparison of the Pb^{206}-$(d,p)Pb^{207}$ angular distributions with the experimental angular distributions for the known Pb^{209} states.

The angular distributions of the major states seen in the (d,p) experiment are plotted in Fig. 6. Several points were reread on the photographic plates and fell within the indicated errors. When no error bars are shown, the error is smaller than the point itself. The number to the right of each angular distribution is the excitation energy of that transition in MeV.

In general, the (d,p) angular distributions show quite a bit of structure, and several possible I^{π} assignments can be made. The single-hole states (Fig. 8) are observed with weaker intensity than the predominately 2h-1p states of Fig. 9. The predicted DWBA angular distributions are plotted with the experimental points on Figs. 8 and 9. The spectroscopic factors given are determined from the curves as drawn and include the normalizing factors of Table III.

The location of the single-hole states in Pb^{207} is well known. These states are excited very strongly in the $Pb^{208}(d,t)$ reaction. In the $Pb^{206}(d,p)$ reaction all six are seen, but the $h_{9/2}$ state at 3.418 MeV is very weak. The spectroscopic factors for this state, as well as for the other single-hole states, are listed in Table I. The DWBA fits for the largest single-hole states shown in Fig. 8 are fair. For the weaker single-hole states, the scatter in the data makes the spectroscopic-factor determination quite uncertain.

Figure 9 compares the experimental angular distributions with the DWBA calculations. One cannot distinguish between the two possible j values for a given l value. However, by keeping in mind the single-particle and single-hole neutron levels (Fig. 1) in the region of interest, one can hope to choose the correct j value and, thus, determine the spectroscopic factor. This was done in Fig. 9 and the probable values are listed in Table I.

The state at 2.728 MeV is one of the strongest in the spectrum. It occurs at an energy where one expects the first 2h-1p state. It is assigned $g_{9/2}$ from this fact and the shape of its angular distribution. With this assignment, the corresponding spectroscopic factor is 0.97. The fit of the $g_{9/2}$ data to the DWBA is fair. One would expect this to be one of the better fits, since it is lowest in energy of any of the 2h-1p states and the intensity of the peak is large. The deviations of the data from the DWBA indicate that only a few definite assignments can be made. This is the reason for several DWBA curves being drawn through each experi-

TABLE IV. States excited in $Pb^{206}(d,p)Pb^{207}$ comparison of present results to those of Hering, Achterath, and Dost (Ref. 12).

E_x (MeV) Present work	E_x (MeV) Ref. 12	J^{π} Ref. 12	Main configuration (Pb^{206} state) ⊗ S.P. state Ref. 12	S Present work	S Ref. 12
2.728	2.73	$\frac{9}{2}^+$	(g.s.)$\otimes g_{9/2}$	0.97	1.16
3.635	3.64	$\frac{5}{2}^+$	$[(2_1^+)\otimes g_{9/2}]_{5/2}$	0.14	0.13
4.319	4.33	$\frac{5}{2}^+$	$[(2_2^+)\otimes g_{9/2}]_{5/2}$	0.19	0.17
4.389	4.40	$\frac{5}{2}^+$	(g.s.)$\otimes d_{5/2}$	0.77	0.61
4.515	4.52	$\frac{5}{2}^+$	$[4_1^+ \otimes g_{9/2}]_{5/2}$	0.08	0.05
4.627	4.64	$\frac{1}{2}^+$	(g.s.)$\otimes s_{1/2}$	1.09	0.84
5.130	5.14	$\frac{7}{2}^+$	(g.s.)$\otimes g_{7/2}$	0.18	0.86
5.181	5.19	$\frac{3}{2}^+$	$[(2_1^+)\otimes d_{5/2}]_{3/2}$	0.25	0.20
5.219	5.23	$\frac{3}{2}^+$	(g.s.)$\otimes d_{3/2}$	0.53	0.67

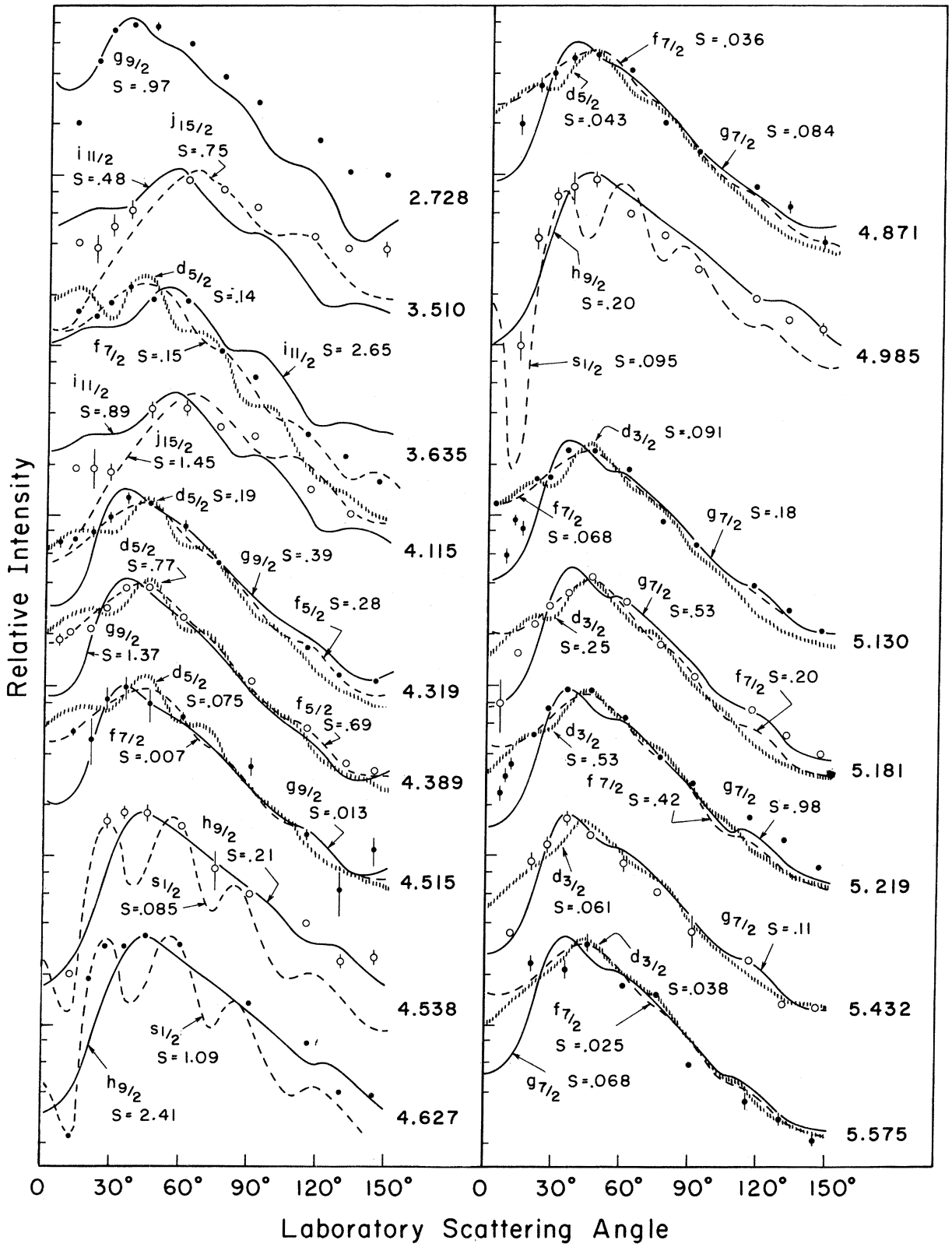

FIG. 9. Angular distributions for the strong transitions observed in $Pb^{206}(d,p)Pb^{207}$. See caption for Fig. 8.

mental angular distribution.

Between the $g_{9/2}$ state at 2.728 MeV and the $d_{5/2}$ state at 4.389 MeV, one expects to see the $i_{11/2}$ and $j_{15/2}$ 2h-1p states. The angular distributions of transitions leading to two states in this region have a broad peak at large angles (45 to 75°) indicative of large l-value transfers. The first, at 3.510 MeV, is probably the $i_{11/2}$ state, as it is about the same distance below the Pb^{209} $i_{11/2}$ as the 2.728-MeV state is below the Pb^{209} $g_{9/2}$. Likewise the state at 4.115 MeV is the proper distance below the Pb^{209} $j_{15/2}$ so it is probably a $j_{15/2}$ state. The spectroscopic factor for the $i_{11/2}$ state is 0.48 and indicates that the single-particle state is somewhat fragmented. The spectroscopic factor for the $j_{15/2}$ (1.45-MeV) state is high by a factor of 2 as discussed in Sec. III A. Thus, it too appears to be fragmented, agreeing with the results for the corresponding state found in Pb^{209}.[9-11]

Previously it was suggested that states at 3.62 and 4.29 MeV[13] were the $i_{11/2}$ and $j_{15/2}$, respectively. As indicated in this work and the work of others,[14,12] these states are $d_{5/2}$ as listed in Table IV at 3.635 and 4.319 MeV.

The angular distribution of the transition leading to the 3.635-MeV state does not resemble either an $l=6$ or 7 and has a spectroscopic factor considerably greater than 1 for either l value. It is probably an $l=2$ transition corresponding to the $g_{9/2}$ neutron coupled to the first 2^+ state of Pb^{206} at 0.803 MeV having a resultant j of $\frac{5}{2}$ as suggested by Hering, Achterath, and Dost.[12] For a comparison of their results to the present work see Table IV. Although the data points are very close to the DWBA calculation for $f_{7/2}$, this assignment is improbable. An $f_{7/2}$ or $f_{5/2}$ state at this energy would probably be a fragment of the single-hole strength, but none is seen at this energy in the $Pb^{208}(d,t)$ reaction, where it should be strongly excited.

The proton angular distributions for transitions to the 4.319- and 4.389-MeV states are very similar. They occur near the energy where one expects the 2h-1p $d_{5/2}$ state. The sum of the spectroscopic factors for these two states (0.96) does not exceed 1. Thus, both are assigned $d_{5/2}$. Reference 12 also assigns both as $d_{5/2}$ with the 4.319-MeV state, the weaker of the two, resulting from the $g_{9/2}$ coupling to the first 4^+ state of Pb^{206} (see Table IV).

Three states are tentatively assigned $s_{1/2}$ based on a sharp forward drop in their proton angular distributions. All three occur in the region where one expects the $s_{1/2}$ to appear. Strongest of these is the 4.627-MeV state, which has a spectroscopic factor of 1.09 and was reported in Ref. 12. The 4.538- and 4.985-MeV states are considerably weaker. As mentioned in Sec. III A, the fact that the sum of the spectroscopic factors is greater than 1 is still within the uncertainty of DWBA calculations.

Transitions to most of the states above 5 MeV in excitation energy (and the 4.871-MeV state) have proton angular distributions which are very similar. These angular distributions peak near 45° and decrease rapidly in the forward direction, but not as fast as do the $s_{1/2}$ angular distributions. The DWBA angular distributions for $l=2$ and 3 are very similar at this energy, while the $l=4$ is peaked slightly more forward and drops off somewhat faster at forward angles.

Several very forward angles (6, 8, 10, 12, 14°) were taken in hopes of distinguishing the $l=4$ an-

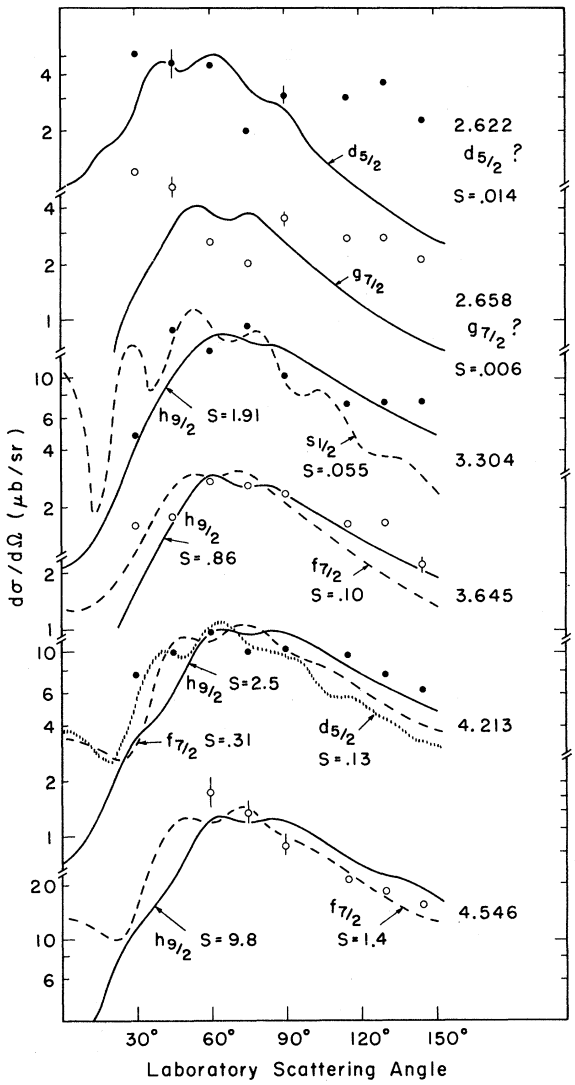

FIG. 10. Fit to DWBA and extracted spectroscopic factors for those transitions of Fig. 7 bearing any similarity to the DWBA curves. Excitation energies in MeV are given on right. Error bars are as in Fig. 7.

gular distributions. Background was very high at 6, 8, and 10° and only the most intense peaks (5.130, 5.181, and 5.219 MeV) could be separated. A broad carbon (d,p) impurity peak obscured several peaks of interest at very forward angles. For those peaks for which data were obtained, the results were inconclusive. The data points lie midway between the $l=2$ and $l=4$ DWBA curves.

The state at 5.130 MeV is assigned by Hering, Achterath, and Dost,[12] Table IV, as $g_{7/2}$. The angular distributions leading to this state and the 5.432-MeV state appear to be slightly more forward peaked than others in this region. However, keeping the agreement between the experimental and DWBA angular distributions of Fig. 9 in mind, one could not definitely assign these states as $g_{7/2}$ based on this work.

Assuming the state at 5.130 is $g_{7/2}$, the discrepancy between the spectroscopic factor obtained in the present work and from Coulomb stripping cannot be easily explained. Table I lists a spectroscopic factor $S=0.18$, whereas Ref. 12 finds $S=0.86$ and Darcey, Jeans, and Jones (DJJ)[14] in their $Pb^{206}(d,p)Pb^{207}$ experiment at 8.0 MeV find $S=1.00$. DJJ mention that the value is unexpectedly high and that additional work is in progress. In the present experiment, this peak is clearly resolved and the normalizing factor of Table III appears normal.

Since the $d_{5/2}$ and $s_{1/2}$ single-particle states are fragmented, one would expect the $g_{7/2}$ and $d_{3/2}$ states, which occur at higher excitation energy, also to be fragmented. Between 5.0 and 5.6 MeV there are many strongly excited states. The largest of these, at 5.219 MeV, is probably $d_{3/2}$. Its spectroscopic factor is 0.53, which would indicate that it is fragmented. Thus, many of the states seen in this region would be components of the $g_{7/2}$ and $d_{3/2}$ single-particle states. Reference 12 assigns the 5.219- and 5.181-MeV states as $d_{3/2}$. Again, since the angular distributions of this work do not allow one to distinguish between $l=2$, 3, or 4 at this energy, no definite assignments can be made.

The three states at 5.057, 5.072, and 5.080 MeV lie very close together. The 5.057-MeV state could generally be separated from the other two, and its proton angular distribution is shown in Fig. 8. The other two states could not be distinguished at all angles. The combined angular distribution indicates that these two states have different l values.

C. $Pb^{208}(d,t)Pb^{207}$

Figure 3 shows the triton spectrum from the $Pb^{208}(d,t)Pb^{207}$ reaction at a laboratory scattering angle of 130°. Although the counts per 0.2 mm are plotted (on a logarithmic scale), data points were read at 0.5-mm intervals because of the poor resolution (FWHM 16–28 keV). The arrows at the bottom of the figure indicate where the 2h-1p states are expected. These states, if seen with the proper j^π value, indicate 2h-2p components in the ground state of Pb^{208}.

At angles greater than 60°, peaks beyond the deuteron elastic [$Pb^{208}(d,d)Pb^{208}$] were observed. The background was quite high (greater than 100 counts) for angles less than 90°. The triton peaks could be distinguished from inelastic deuteron peaks by their relative shift with angle. No large inelastic deuteron peaks were observed. The first inelastic deuteron state in Pb^{208} is at 2.615 MeV, which would occur at a distance along the plate of 3.83 cm.

The states at 4.546 and 4.311 MeV (not shown in Fig. 3) are obscured at several angles by the shifting deuteron elastic peak. In addition, there may be one or two peaks at approximately 4.386 and 4.373 MeV which were only seen at two or three angles because of the deuteron elastic peak.

The peak due to excitation of the $f_{7/2}$ single-hole state at 2.339 MeV is too dense to be read on the exposure of Fig. 3. Shorter exposures were made to obtain angular distributions for this state and other over-exposed single-hole states shown in Fig. 12. The $h_{9/2}$, weakest of the single-hole states (the strongest are 40 times stronger), is shown here at 3.415 MeV with excellent intensity.

The angular distributions for tritons exciting the single-hole states of Pb^{207} are shown in Fig. 12. The solid-line curves shown are calculated by DWBA. These fits are quite good, although no attempt was made to improve the parameters taken from Ref. 7. The horizontal lines near the top of the angular distributions indicate the expected intensity corresponding to spectroscopic factors equal to $(2j+1)$. These values for the spectroscopic factors would imply that these states are completely of single-hole character – corresponding to removal of a neutron from a full shell.

Figure 7 shows the experimental triton angular distributions leading to states above 2.339 MeV in excitation in Pb^{207}. The DWBA curves for the highest single-hole states and the 2h-1p states are shown on the right side of Fig. 7 for comparison. The lack of low-angle data above 4.4 MeV is due to the high background from the elastic deuteron peak.

A very surprising feature of Fig. 7 is the lack of similarity between the experimental and the DWBA angular distributions. These states are excited with good intensity and the experimental angular distributions should be quite reliable. Only the transitions leading to the 2.725-, 3.304-, 3.645-, 4.213-, and 4.546-MeV states have angular distri-

butions which bear any similarity to the DWBA angular distributions. The rest of the angular distributions either remain flat or increase with lower or higher angles, which is contrary to the shape of the DWBA angular distributions. These states probably arise from a reaction mechanism other than a direct pickup. Perhaps this mechanism is a two-step process. The intensity of these states (about 1000 times weaker than the single-hole states) is near the expected magnitude for a two-step process.[15]

In Fig. 10, the DWBA curves are drawn through the data points and the extracted spectroscopic factors are given for some of the states above 2.339 MeV.

The first two angular distributions are for the collective 3^- core excited state of either Pb^{206} or Pb^{208} coupled to the $p_{1/2}$ ground state of Pb^{207}, so these states must be $\frac{5}{2}^+$ and $\frac{7}{2}^+$. The (d,t) angular distributions leading to these states appear somewhat similar, but nothing like $d_{5/2}$ or $g_{7/2}$. Perhaps with such a low differential cross section (<6 μb/sr), these states are being excited via mechanisms other than direct pickup.

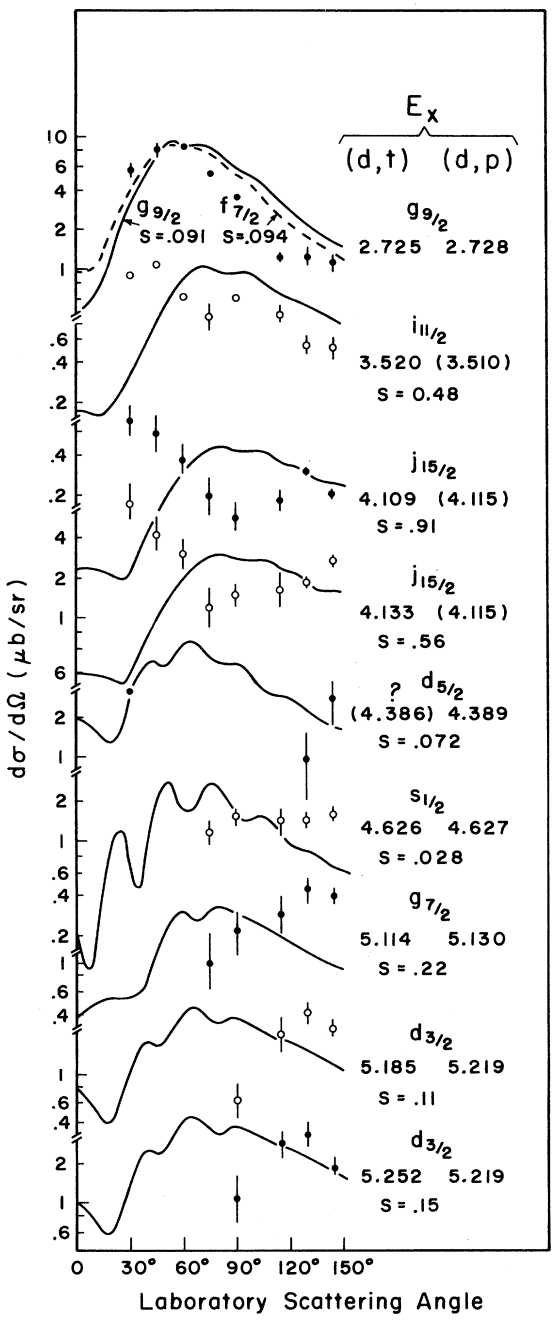

FIG. 11. Search for the 2h-1p states in the $Pb^{208}(d,t)$-Pb^{207} reaction. Curves through the data points and spectroscopic factors are calculated from DWBA. Transitions shown are those closest in excitation energy (shown on the right) to the 2h-1p states observed in the Pb^{206}-$(d,p)Pb^{207}$ reaction.

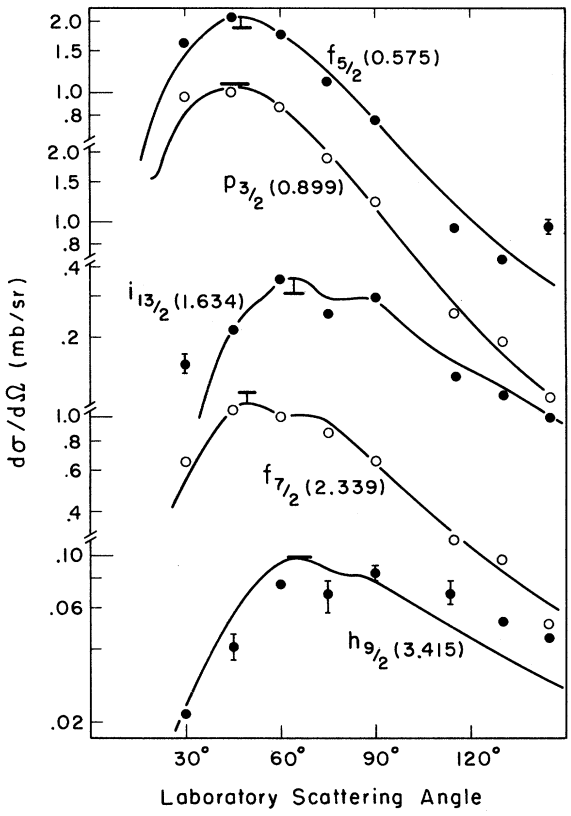

FIG. 12. Experimental and DWBA triton angular distributions for transitions leading to the single-hole states excited in $Pb^{208}(d,t)Pb^{207}$. Numbers in parentheses are excitation energies in MeV. The curves through the data points are the calculated DWBA angular distributions. Horizontal lines near the top of each curve indicate intensities corresponding to spectroscopic factors with a value of $(2j+1)$. The $p_{1/2}$ ground state was not on the plate for all angles and is not shown.

The state at 3.304 MeV was reported to be weakly excited at 3.29 MeV in a recent $Pb^{208}(p,d)Pb^{207}$ reaction at 40 MeV by Smith, Roos, Moazed, and Bernstein.[16] They tentatively assign it $l=0$ with $j^{\pi}=\frac{1}{2}^{+}$ arising from the coupling of an $f_{5/2}$ neutron hole to the 3^{-} state of Pb^{208}. Although the angular distribution shown in Fig. 10 is far from conclusive, it does have some characteristics of an $l=0$ transition. Typically such distributions have a sharp forward minimum and remain high for a large angular range. If this is an $s_{1/2}$ state, then its spectroscopic factor is 0.055.

Smith *et al.*[16] suggest the other components of the $(f_{5/2}\times 3^{-})_j$ multiplet might be contained in what they call an unresolved doublet at 3.19 MeV. In this work, three states are seen in this region – 3.180, 3.202, and 3.224 MeV. The angular distributions of tritons leading to these states are unlike any of the DWBA curves.

The state at 4.546 MeV is the strongest state in the spectrum aside from the single-hole states. The angular distribution is not complete, since at forward angles this peak was obscured by the elastic deuteron peak. This state was tentatively assigned as $f_{7/2}$ by Yagi *et al.*[17] Recently, Smith *et al.*[16] have also assigned this state as $f_{7/2}$ with about 10% of the $f_{7/2}$ single-hole-state strength. Fitting the backward-angle data (Fig. 10), a spectroscopic factor of approximately 1.40 is obtained. This corresponds to 17% of the total expected strength. This value is a little more than is missing from the 2.339-MeV state, but still within the experimental error. The error may be larger for this state, since the maximum was not observed in the angular distribution.

The $h_{9/2}$ DWBA angular distribution is drawn through the data points for the 3.304-, 3.645-, 4.213-, and 4.546-MeV states in Fig. 10, since it has been suggested[16,18-20] that the $h_{9/2}$ single-hole state is also fragmented. The spectroscopic factor found in this work, 9.75 for the $h_{9/2}$ state at 3.415 MeV, is close to the unfragmented value; however, it cannot be said to rule out fragmentation. Certainly, the value for the 4.546-MeV state ($S=9.84$) is much too large, so this state is not a $h_{9/2}$ fragment.

Transitions to the 3.645- and 4.213-MeV states have triton angular distributions which do not allow definite l-value assignments. Although the angular distribution dips at forward and backward angles, the entire distribution remains quite flat. Thus, these transitions may not correspond to a single-step pickup reaction mechanism.

Figure 11 shows the angular distributions for transitions in the $Pb^{208}(d,t)Pb^{207}$ reaction leading to states which are close in energy to the 2h-1p states seen in $Pb^{206}(d,p)Pb^{207}$. The DWBA triton angular distributions are fitted to the data and the extracted spectroscopic factors are given.

For several of the states the difference between the (d,t) and (d,p) energies is quite large. Based on a linear interpolation of the deviation in (d,p) and (d,t) energies below the normalizing energy of 2.3393 MeV, one expects the (d,t) energies to be lower than the (d,p) energies for states above 2.3393 MeV. This deviation could be as much as 5 to 8 keV at 5.6-MeV excitation. Hence, those states in Fig. 11 with (d,t) energies higher than (d,p) or with energy differences of more than 8 keV probably do not correspond to the 2h-1p states seen in $Pb^{206}(d,p)Pb^{207}$.

Table V lists the amount of upper limit of the 2h-2p components in the ground state of Pb^{208}. The ground state of Pb^{208} can be written

$$Pb^{208}\text{g.s.} = \text{closed shell} + a\,Pb^{206}(g_{9/2})^2 + b\,Pb^{206}(i_{11/2})^2 + \cdots ,$$

where "Pb^{206}" indicates the two-hole configuration belonging to Pb^{206} and $(l_j)^2$ indicates the two particles of orbital angular momentum l and total angular momentum j added to the Pb^{206} configuration. The coefficient squared is calculated from the spectroscopic factors for the (d,p) and (d,t) 2h-1p states

$$(\text{Coeff.})^2 = \frac{1}{2}\frac{S(d,t)}{S(d,p)}.$$

If the spectroscopic factor is unity in the (d,p) reaction, then the fraction of that component in the ground state of Pb^{208} is $\frac{1}{2}$ the spectroscopic factor seen in the (d,t) experiment (since there are two particles in this state). If the (d,p) spectroscopic factor is less than unity, then the coefficient must be increased by that amount.

The triton angular distribution leading to the 2.725-MeV state in Pb^{207} is quite close to the $g_{9/2}$ DWBA angular distribution. The $f_{7/2}$ DWBA curve also fits the data points; however, this state is 3 keV below the $g_{9/2}$ 2h-1p state seen in the $Pb^{206}(d,p)$ reaction. There can be little doubt that the state seen in (d,t) is the 2h-1p state and thus corresponds to a 2p-2h component in the ground state of Pb^{208} as previously reported.[21]

The closest peak in Fig. 3 to the expected position of the 2h-1p $i_{11/2}$ state is at 3.520 MeV. Comparing the energy between the (d,p) and (d,t) on Fig. 11, one finds that the peak in the (d,t) reaction is higher by 10 keV. This energy shift is too large and in the wrong direction to associate the (d,t) level with the probable $i_{11/2}$ seen in the (d,p) reaction. The angular distribution for tritons leading to this state does not fit the $i_{11/2}$ DWBA curve.

For these reasons, an upper limit is listed in Table V for the possible 2h-2p (Coeff.)^2 in the ground state of Pb^{208}. The value of the upper limit, taken from the expected location of the 2h-1p state, is large because of the proximity of the 3.520-MeV state.

The expected location of the $j_{15/2}$ 2h-1p state lies in the valley between two closely spaced peaks. Both angular distributions are plotted and compared with the DWBA curves in Fig. 11. Neither angular distribution bears any similarity to the DWBA. The energy difference between the (d,p) and (d,t) is larger than expected. Again the upper limit listed in Table V is based on the expected location of the $j_{15/2}$ state tentatively assigned in the (d,p) work.

Only three data points were obtained for the possible $d_{5/2}$ 2h-1p state. This peak is obscured by the deuteron elastic peak at all angles except 30, 130, and 144°. At the backward angles, it is on the tail of the deuteron elastic peak and its differential cross section is uncertain, as indicated by the large error bars in Fig. 11. The energy of this state is quite close to that of the 2h-1p state excited in the $Pb^{206}(d,p)$ reaction. The theoretical DWBA curve is drawn through the data in Fig. 11 and the value for the (Coeff.)^2 is listed in Table V.

The $s_{1/2}$, $g_{7/2}$ and $d_{3/2}$ 2h-1p states are expected at an energy below the deuteron elastic. Thus, no forward-angle data are available for these states.

The 4.626-MeV state in $Pb^{208}(d,t)$ occurs very close to the energy expected for the $s_{1/2}$ 2h-1p state. The angular distribution leading to this state is fairly flat and follows the DWBA poorly. If this state does correspond to a 2h-2p component in the ground state of Pb^{208}, the (Coeff.)^2 would be 1.3%.

The expected locations of the $g_{7/2}$ and $d_{3/2}$ 2h-1p states in $Pb^{208}(d,t)$ both fall on the edges of peaks. These states in (d,t) have too large an energy difference from the 2h-1p states excited in $Pb^{206}(d,p)$ to be considered 2h-1p states. The upper limits quoted in Table V are obtained from the expected location of the 2h-1p states and not the angular distributions plotted in Fig. 11.

TABLE V. 2h-2p components in the ground state of Pb^{208}, assuming Pb^{208} ground state to be of the form

$$Pb^{208}\text{g.s.} = \text{c.s.} + a\,Pb^{206}(g_{9/2})^2 + b\,Pb^{206}(i_{11/2})^2 + \cdots .$$

Component	(Coeff.)^2	Fit to angular distribution
$Pb^{206}(g_{9/2})^2$	0.047 ± 0.007	Fair
$Pb^{206}(i_{11/2})^2$	<0.20	No peak
$Pb^{206}(j_{15/2})^2$	<0.21	No peak
$Pb^{206}(d_{5/2})^2$	$\gtrsim 0.047 \pm 0.023$	Only 3 pts.
$Pb^{206}(s_{1/2})^2$	$\lesssim 0.013 \pm 0.013$	Poor
$Pb^{206}(g_{7/2})^2$	<0.25	No peak
$Pb^{206}(d_{3/2})^2$	<0.03	No peak

Table V summarizes the search for 2h-2p components in the ground state of Pb^{208}. The possible errors listed in Table V correspond to uncertainty in the experimental cross sections and data points. Any possible error in spectroscopic-factor extraction based on DWBA cross sections is not included.

For those states for which a (Coeff.)^2 can be determined, the 2h-2p components in the ground state of Pb^{208} are quite small. This implies that the Pb^{208} neutron "core" is quite closed. Deviations from the closed shell are only a few percent.

The results of this paper are consistent with the reported values for 2h-2p components in the ground state of Pb^{208}. Smith *et al.* in their $Pb^{208}(p,d)Pb^{207}$ reaction at 40 MeV have reported[16] seeing the $g_{9/2}$ 2h-1p state at 2.74 MeV with a spectroscopic strength of 0.05 ± 0.02. This they say corresponds to 2–4% $Pb^{206}(g_{9/2})^2$ component in the Pb^{208} ground state. Parkinson *et al.*[22] have set an upper limit on the strength of the $g_{9/2}$ level at 2.73 MeV seen in their $Pb^{208}(d,t)Pb^{207}$ reaction at 50 MeV which would correspond to a 5% admixture into the Pb^{208} ground state. The energies of the 2h-1p states in Pb^{207} excited from Pb^{206} were not determined in either of the above experiments. Thus, no direct comparison was made between stripping and pick-up reactions as in the present experiment.

D. $Pb^{207}(d,d')Pb^{207}$

Only three angles were exposed in the (d,d') experiment. This experiment was performed to have a third independent method of determining the Pb^{207} energy levels. Since only excitation energies were of interest in this experiment, no attempt was made to obtain complete angular distributions.

A typical spectrum is shown in Fig. 4. The collective $\frac{5}{2}^+$ and $\frac{7}{2}^+$ states are seen in a shorter exposure (indicated by the dashed lines) at 2.622 and 2.657 MeV, respectively. Several states were probably missed because of the high level density and high background. Some isotopic impurities may have been included in this experiment because of the extremely high level density in the Pb^{NAT}-(d,d') reaction, which was used to eliminate such impurities. A number of uncertain states near 4.7 MeV are indicated by parentheses around their excitation energies. The shifting C^{12} ground state obscured these peaks at 75°, so peak assignments for these states are based on only two angles.

The assignments shown in Fig. 5 are made by comparing the present (d,d') results with the Pb^{207}-$(p,p')Pb^{207}$ work of Vallois[5] at 24.5 MeV. The energies of that work are also included in Table I.

The discrepancy between the energies of Ref. 5 and those of the present work is surprising. It may be due to the better resolution of this experiment [several (p,p') peaks were resolved as doublets in this work] or to the uncertainty in the energy of the impurity peaks which were used in Ref. 5 to determine an energy calibration.

IV. SUMMARY

Table I lists all states seen in the three reactions considered in this work. Also listed are the maximum differential cross sections, I^π assignments, and spectroscopic factors. The lack of distinctive structure in both the $Pb^{206}(d,p)Pb^{207}$ and the $Pb^{208}(d,t)Pb^{207}$ reactions prohibited the assignment of more I^π values than are listed in Table I.

The 2h-1p states seen in the (d,p) reaction seem to be fragmented at high excitation energies. Tentative assignment of the missing $i_{11/2}$ and $j_{15/2}$ states at 3.510 and 4.115 MeV was made. The core excited weak-coupling model works very well for several states excited in the $Pb^{206}(d,p)Pb^{207}$ reaction, as shown in Table IV.

As can be seen from Table V, the 2h-2p components (assuming a one-step process) in the ground state of Pb^{208} are small. This indicates that Pb^{208} is a very good closed-shell nucleus.

Further indication of this is apparent from the lack of similarity between states excited in the (d,p) and (d,t) reactions. Pb^{208} is a much better closed-shell nucleus than the lighter closed-shell nuclei, where admixtures in the ground state are much larger.

The flatness of the (d,t) experimental angular distribution may imply that these weak states (generally less than 5 μb/sr) are excited in some reaction other than direct pickup – perhaps a two-step process.

Recently a high-resolution $Bi^{209}(d,\alpha)Pb^{207}$ reaction at 17 MeV has been performed using the University of Pittsburgh Enge split-pole spectrograph.[23] Using an independent spectrograph calibration, many of the levels seen in that work agree within 3 to 4 keV with the levels seen in the (d,p) and (d,t) reactions reported here. This supports the contention that the lack of line-up between the (d,p) and (d,t) is real. A state at the energy expected for the 2h-1p $g_{9/2}$ state is seen in the (d,α) reaction.

---

*Research supported by the National Science Foundation.

†Present address: Nuclear-Chicago Corporation, Des Plaines, Illinois 60018.

‡Present address: Mobil Research and Development Corporation, Paulsboro, New Jersey 08066.

[1]D. A. Bromley and J. Weneser, Comments Nucl. Particle Phys. 2, 151 (1968).

[2]N. Stein, in *Proceedings of the International Conference on Properties of Nuclear States, Montréal, Canada, 1969,* edited by M. Harvey *et al.* (Presses d l' Université de Montréal, Montréal, Canada, 1969), p. 337.

[3]B. L. Cohen, J. B. Moorhead, and R. A. Moyer, Phys. Rev. 161, 1257 (1967).

[4]J. B. Marion and F. C. Young, *Nuclear Reaction Analysis* (North-Holland Publishing Company, Amsterdam, The Netherlands, 1968), p. 145.

[5]G. Vallois, Commissariat a l' Energie Atomique Report No. CEA-R-3500, 1968 (unpublished).

[6]R. H. Bassel, R. M. Drisko, and G. R. Satchler, Oak Ridge National Laboratory, Memorandum on Code JULIE (unpublished).

[7]G. Muehllehner, A. S. Poltorak, W. C. Parkinson, and R. H. Bassel, Phys. Rev. 159, 1039 (1967).

[8]P. Mukherjee and K. V. Chalapati Rao, private communication.

[9]G. J. Igo, P. D. Barnes, E. R. Flynn, and D. D. Armstrong, Phys. Rev. 177, 1831 (1969).

[10]C. Ellegaard, H. Kantele, and P. Vedelsby, Nucl. Phys. A129, 113 (1969).

[11]W. R. Hering and H. Rudolph, Bull. Am. Phys. Soc. 15, 547 (1970).

[12]W. R. Hering, A. D. Achterath, and M. Dost, Phys. Letters 26B, 568 (1968).

[13]P. Mukherjee and B. L. Cohen, Phys. Rev. 127, 1284 (1962).

[14]W. Darcey, A. F. Jeans, and K. N. Jones, Phys. Letters 25B, 599 (1967).

[15]P. J. Iano and N. Austern, Phys. Rev. 151, 853 (1966).

[16]S. M. Smith, P. G. Roos, C. Moazed, and A. M. Bernstein, private communication.

[17]K. Yagi, Y. Ishimatsu, Y. Ishizaki, and Y. Saji, Nucl. Phys. A121, 161 (1968).

[18]I. Hamamoto, Nucl. Phys. A141, 1 (1970).

[19]W. P. Alford and D. G. Burke, Phys. Rev. 185, 1560 (1969).

[20]C. A. Whitten, Jr., N. Stein, G. E. Holland, and D. A. Bromley, Phys. Rev. 188, 1941 (1969).

[21]R. A. Moyer, B. L. Cohen, and R. C. Diehl, Bull. Am. Phys. Soc. 14, 510 (1969).

[22]W. C. Parkinson, D. L. Hendrie, H. H. Duhm, J. Mahoney, and J. Saundinos, Phys. Rev. 178, 1976 (1969).

[23]C. Ellegaard, private communication.